Sparse Damage Localization Using Lamb Waves Based on a Finite Element Model

Pan Pan†, Yiyin Wang†, Fucai Li*, Cailian Chen†, and Xinping Guan†

†Department of Automation, Shanghai Jiao Tong University, Shanghai, 200240, P. R. China
*State Key Laboratory of Mechanical System and Vibration, Shanghai Jiao Tong University, Shanghai, 200240, P. R. China

***Abstract*—In this paper, we propose a damage localization method exploiting the spatial sparsity of the damages for an isotropic aluminium plate. The proposed method not only makes use of Lamb-wave responses measured by a wireless sensor network (WSN), but also takes advantage of the wave propagation model, which governs the physical characteristics of the Lamb-waves. The finite element method (FEM) is applied to approximate the wave propagation model. The resulted linear system model is combined with WSN measurements to formulate an inverse problem for damage localization. The ℓ_1 regularization is employed to solve the inverse problem and exploit the spatial sparsity of the damages. The simulation results illustrate the efficiency of the proposed algorithm.**

***Index Terms*—Damage localization, Lamb wave, finite element model, inverse problem, sparsity**

I. Introduction

Damage identification finds numerous applications in structural engineering to preserve integrity and safety of structures [1, 2]. It aims to identify a structural damage at early stage by measuring the dynamic response of the observed system and evaluating its health status. In traditional Lamb-wave based damage identification systems, one of the most important drawbacks is that a number of transducers must be used to construct a wired sensor network, which complicates the systems. Furthermore, wires and connectors may influence the structures under test. Hence, wireless sensor networks (WSNs) can be an appropriate selection for practical damage identification applications. With the advances of WSNs, damage identification evolves to a stage where continuous monitoring can be accomplished in a cost-efficient way [3]. Among different interrogating signals, Lamb waves can propagate over a long distance, and are highly sensitive to inhomogeneity and abnormalities of structures [4]. Therefore, a promising scheme for damage identification is via analyzing the Lamb-wave response collected by a WSN.

In general, damage identification methods can be categorized as response-based or model-based ones. The first kind of methods only depends on response measurements. They either exploit the correlation between pairwise signals or extract time-of-flights of interrogating signals [4–6]. Although these methods are computationally efficient, their estimation accuracy is limited due to the absence of the structural characteristics. On the other hand, the model-based methods [7, 8] not only make use of measurements, but also take benefit of structural models, which reveal physical properties of structures. Most model-based methods belong to the sensitivity-type [8], which is based on a parametric model and a cost function of the errors between the measurements and the predictions from the model. These model-based methods provide solutions to damage identification, which can be viewed as an inverse problem.

Damage identification usually involves four levels, including detection, localization, quantification, and prediction [8]. In this paper, we focus on damage localization on an isotropic aluminium plate, and propose an inverse algorithm for damage localization using Lamb-wave responses collected by a WSN. The simple plate structure is employed, as it is fundamental for complicated structures. The proposed algorithm belongs to the sensitivity-type model-based methods. Most traditional methods extract system models from the law of motion [9], acquire the *stiffness* and *mass* matrices, and perform model updating. The process of model updating takes large amount of calculation and makes algorithms inefficient for empirical testing. On the other hand, we propose a system model based on the primary propagation law [10]. Since the isotropic structure is a perfect wave guide, a damage that scatters incident waves can be approximately modeled as an extended exciting source according to the wave propagation law. The system model is numerically approximated by the finite element method (FEM) [11]. The damage related parameters are linearly related to the measurements in the system model and we do not need to update the model step by step, in other words, the computation complexity is reduced. Since the damages are sparsely distributed on the plate under testing, the ℓ_1 regularized least squares estimator is proposed for damage localization.

The outline of the rest of the paper is as follows. In Section II, the system model in the frequency domain based on the wave propagation law is introduced. The impact of the damages is approximated as exciting sources. The observation model constructed with the WSN is also given. A detailed finite element analysis of the system model is shown in Section III. As a result, an approximated linear model is obtained. In Section IV, the sparsity of the damages are used to solve the inverse problem based on the approximated linear model. Numerical results are illustrated in Section V. Conclusions are

978-1-4799-7339-2/14/$31.00 ©2014 IEEE

drawn in Section VI.

II. System model

In this paper, we consider damage localization on an isotropic aluminium plate, where a WSN is deployed to measure the Lamb-wave response excited by tone bursts [12]. The damages are the discontinuous or inhomogeneous regions of the structure. Moreover, the damages are assumed to be small and spatially sparse compared to the whole area under test. Piezo-electrical sensors are employed by the WSN to excite or measure Lamb-wave signals. All the data measured by the sensors is collected by a fusion center, where damage localization is carried out.

A. The wave propagation model

It is well known that wave propagation in solid media have special multimodal and dispersive features [5, 6, 10]. Lamb waves in plate-like structures result from the superposition of guided longitudinal and transverse shear waves within an elastic layer. There are two groups of waves, namely symmetric and anti-symmetric waves, and each can propagate independently of the other. The Rayleigh-Lamb frequency equations for the propagation of symmetric and anti-symmetric waves in a plate are given, respectively [10]

$$\frac{\tan(qh)}{\tan(ph)} = -\frac{4k^2pq}{(q^2-k^2)^2}, \tag{1}$$

$$\frac{\tan(qh)}{\tan(ph)} = -\frac{(q^2-k^2)^2}{4k^2pq}, \tag{2}$$

where h is the half-thickness of the plate, k is the wavenumber, p and q are given as $p^2 = w^2/c_L^2 - k^2$ and $q^2 = w^2/c_T^2 - k^2$ (ω is the angular frequency), respectively, and c_L and c_T are the velocities of longitudinal and transverse bulk waves in the plate, respectively. They are determined by the density, Young's modulus and Poisson's ratio of the plate material.

For a typical frequency, several wave modes coexist, and each mode has a corresponding propagating velocity. These features usually make wave signals complex to interpret and analyze. To relieve the complexity, we consider the propagation model of a single-mode wave in frequency domain. Note that we deal with the single-model signal, while the actual wave field is the superposition of multiple modes. Hence, the preprocessing methods are required to separate the composite signal into the single-mode signals. There are various options to accomplish the mode separation [13, 14]. Therefore, we take benefit of these methods, and assume that the preprocess is accomplished and the signal-mode signal is available.

Let us assume that the mth wave mode is used. We define a two-dimensional area of interest Ω as the top surface of an aluminum plate, $\mathbf{x}$ as a casual position of Ω, $u_m(\mathbf{x},\omega)$ as the mth mode field value at frequency ω and position $\mathbf{x}$, $s_m(\mathbf{x},\omega)$ as the mth mode driving force at frequency ω and position $\mathbf{x}$, and $k_m(\omega)$ as the frequency and mode dependent wavenumber. The system model is given by the Helmholtz equation [10] as

$$\nabla^2 u_m(\mathbf{x},\omega) + k_m^2(\omega)u_m(\mathbf{x},\omega) = s_m(\mathbf{x},\omega). \tag{3}$$

The above partial differential equation (PDE) describes the physical characteristics of a single-mode wave propagation in frequency domain. As the PDE (3) only describes an intact plate, we now introduce damages into the system model. In the area Ω, the damages are assumed to be closely bounded by the boundary curve C, and they are linear damages. When the incident waves propagate to the boundary C, they would be reflected or refracted by the damages. As a result, according to the Huygens-Fresnel principle, the total wave field $\widetilde{u}_m(\mathbf{x},\omega)$ is the proposition of the incident field $u_m(\mathbf{x},\omega)$ and the scattered field $v_m(\mathbf{x},\omega)$ [15]

$$\widetilde{u}_m(\mathbf{x},\omega) = u_m(\mathbf{x},\omega) + v_m(\mathbf{x},\omega). \tag{4}$$

The total wave field $\widetilde{u}_m(\mathbf{x},\omega)$ is governed by the Helmholtz equation as well

$$\nabla^2\widetilde{u}_m(\mathbf{x},\omega) + \widetilde{k}_m^2(\mathbf{x},\omega)\widetilde{u}_m(\mathbf{x},\omega) = s_m(\mathbf{x},\omega), \tag{5}$$

where $\widetilde{k}_m(\mathbf{x},\omega)$ is the wavenumber for the total field.

In general, the scattering process is difficult to obtain an analytical solution, but can be approximated by computing a boundary value problem. When the incident waves propagate to the boundaries of the damages, there would be complex phenomena, such as scattering, amplitude deduction and sometimes even wave mode conversion [16, 17]. Chaillat et al. modeled this process by adding a perturbation on the wavenumber at the boundaries of the damages [18] as

$$\widetilde{k}_m^2(\mathbf{x},\omega) = \begin{cases} k_m^2(\omega) + \eta_m(\mathbf{x},\omega), & \mathbf{x}\in C \\ k_m^2(\omega), & \mathbf{x}\notin C,\ \mathbf{x}\in\Omega \end{cases}, \tag{6}$$

where $k_m(\omega)$ is the wavenumber of the chosen exciting tone burst with reference to structure material, $\eta_m(\mathbf{x},\omega)$ is the perturbation defined on the casual position $\mathbf{x}$ at frequency ω for the mth mode incident wave on the boundary C. Thus, $\eta_m(\mathbf{x},\omega)$ closely relates to the location and feature of the damages.

Introducing (4) and (6) into (5), making use of (3), and using the Born approximation [19], the scattered field of the mth mode can be modeled as

$$\nabla^2 v_m(\mathbf{x},\omega) + k_m^2(\omega)v_m(\mathbf{x},\omega) \approx -\eta_m(\mathbf{x},\omega)u_m(\mathbf{x},\omega), \tag{7}$$

The product at the right side of (7) is aggregated as a single term $f_m(\mathbf{x},\omega)$ as

$$f_m(\mathbf{x},\omega) \triangleq \begin{cases} -\eta_m(\mathbf{x},\omega)u_m(\mathbf{x},\omega), & \mathbf{x}\in C \\ 0, \quad \text{otherwise} \end{cases}, \tag{8}$$

where $f_m(\mathbf{x},\omega)$ can be viewed as an equivalent source of a single-mode perturbation at the boundaries of the damages, and it has a limited spatial support related to the damage locations. Thus, the scattered field can be modeled by the approximated source term $f_m(\mathbf{x},\omega)$ as

$$\nabla^2 v_m(\mathbf{x},\omega) + k_m^2(\omega)v_m(\mathbf{x},\omega) = f_m(\mathbf{x},\omega) + e(\mathbf{x},\omega), \tag{9}$$

where $e(\mathbf{x},\omega)$ is the model fitting error. The above equation is the PDE model describing the relationship between $v_m(\mathbf{x},\omega)$ and $f_m(\mathbf{x},\omega)$, and would be used for damage localization.

B. The observation model

Assume that J sensors are located on the plate surface at positions $\mathbf{x}_j,\ j = 1, 2, ..., J$. For a typical frequency ω and the mth wave mode, the observation model can be written as

$$\bar{v}_m(\mathbf{x}_j, \omega) = v_m(\mathbf{x}_j, \omega) + n(\mathbf{x}_j, \omega), \tag{10}$$

where $\bar{v}_m(\mathbf{x}_j, \omega) = \bar{\widetilde{u}}_m(\mathbf{x}_j, \omega) - \bar{u}_m(\mathbf{x}_j, \omega)$ with $\bar{\widetilde{u}}_m(\mathbf{x}_j, \omega)$ and $\bar{u}_m(\mathbf{x}_j, \omega)$ being the field measurements of the damaged ($\widetilde{u}_m(\mathbf{x}_j, \omega)$) and the intact plate ($u_m(\mathbf{x}_j, \omega)$), respectively. The term $v_m(\mathbf{x}_j, \omega)$ is the same as the one defined in (4), and represents the scattered wave field of the mth mode at position $\mathbf{x}_j$ and frequency ω, and $n(\mathbf{x}_j, \omega)$ is the additive Gaussian white noise (AWGN). The measurements are transmitted within the WSN, and collected by the fusion center.

III. The FEM approximation

In the previous section, the wave propagation model (the PDE model) as well as the observation model are introduced. However, it is difficult to obtain an exact analytical solution for such PDE models. This is one of the main reasons that many methods neglect the system model, and only focus on statistical models directly from measured data. Nevertheless, the PDE models are rich in information about the structures, and can contribute to damage identification. Furthermore, computation complexity is another issue that should be taken into account. Thus, we resort to the numerical methods to approximately transform the original PDE model into a linear model with finite dimensions. In this paper, the classical finite element method (FEM) is employed for this purpose.

First, the area Ω is discretized by a dense mesh with N mesh points. The mesh points are selected to be evenly placed all over the whole surface, and their mean distance is small enough to accurately approximate the wave field. The denser the mesh points are, the better accuracy the approximation can be achieved. Second, the Galerkin equations [11] are introduced to represent the scattered field $v_m(\mathbf{x}, \omega)$ and the aggregate source $f_m(\mathbf{x}, \omega)$ at the casual positions $\mathbf{x}$ as the linear interpolation of the values at the mesh points [11]

$$v_m(\mathbf{x}, \omega) = \sum_{i=1}^{N} v_m(\mathbf{x}_i, \omega)\varphi_i(\mathbf{x}), \tag{11}$$

$$f_m(\mathbf{x}, \omega) = \sum_{i=1}^{N} f_m(\mathbf{x}_i, \omega)\varphi_i(\mathbf{x}), \tag{12}$$

where $\mathbf{x}_i$ is the position where the ith mesh point locates, and $\varphi_i(\mathbf{x})$ is the basis function of the approximated solution space. In order to maintain the orthogonality and completeness of the space, $\varphi_i(\mathbf{x})$ is chosen to be positive semi-definite around $\mathbf{x}_i$ within only a very limited spatial area and zero elsewhere. Various basis functions are available according to different requirements [11]. We make use of the Lagrange triangular finite element in this paper.

The second order Laplace operator ∇^2 in (9) is difficult to handle, thus a numerical method is used to split it off. Let us multiply a test function $g(\mathbf{x})$ at both sides of (9), and take the integration over the whole area Ω. The test function can be arbitrary in the space formed by the basis functions but should not be zero. As a result, we arrive at

$$\begin{aligned} &\iint_{\Omega} k_m^2(\omega) v_m(\mathbf{x}, \omega) g(\mathbf{x}) dxdy \\ &+ \iint_{\Omega} \nabla^2 v_m(\mathbf{x}, \omega) g(\mathbf{x}) dxdy = \iint_{\Omega} f_m(\mathbf{x}, \omega) g(\mathbf{x}) dxdy. \end{aligned} \tag{13}$$

According to the Green's formula [11], (13) can be rewritten as

$$\begin{aligned} &k_m^2(\omega) \iint_{\Omega} v_m(\mathbf{x}, \omega) g(\mathbf{x}) dxdy \\ &- \iint_{\Omega} \nabla v_m(\mathbf{x}, \omega) \nabla g(\mathbf{x}) dxdy = \iint_{\Omega} f_m(\mathbf{x}, \omega) g(\mathbf{x}) dxdy. \end{aligned} \tag{14}$$

We remark that we neglect the boundary reflection from the edge of the plate, as the interested wave signals are only captured before the arrival of the boundary-reflected waves. This assumption is valid, if the plate is large enough or the reflection noise can be suppressed in preprocessing procedure. It is the reason that we omit an integral term, which computes the integration at the edge of the plate in (14). Note that the operator ∇^2 has been replaced, and the computational difficulty is reduced. For the test function, it can also be written as the summation of the basis functions according to the Galerkin method

$$g(\mathbf{x}) = \sum_{i=1}^{N} \varphi_i(\mathbf{x}). \tag{15}$$

Plugging (11), (12), and (15) into (14), we achieve

$$\begin{aligned} &- \iint_{\Omega} \nabla \sum_{i=1}^{N} v_m(\mathbf{x}_i, \omega)\varphi_i(\mathbf{x}) \nabla \sum_{k=1}^{N} \varphi_k(\mathbf{x}) dxdy \\ &+ k_m^2(\omega) \iint_{\Omega} \sum_{i=1}^{N} v_m(\mathbf{x}_i, \omega)\varphi_i(\mathbf{x}) \sum_{k=1}^{N} \varphi_k(\mathbf{x}) dxdy \\ &= \iint_{\Omega} \sum_{i=1}^{N} f_m(\mathbf{x}_i, \omega)\varphi_i(\mathbf{x}) \sum_{k=1}^{N} \varphi_k(\mathbf{x}) dxdy. \end{aligned} \tag{16}$$

As the orthogonal basis functions are used, and the sequence of the operators are changeable, we arrive at

$$\begin{aligned} &- \sum_{i=1}^{N} v_m(\mathbf{x}_i, \omega) \sum_{k=1}^{N} \iint_{\Omega} \nabla\varphi_i(\mathbf{x}) \nabla\varphi_k(\mathbf{x}) dxdy \\ &+ k_m^2(\omega) \sum_{i=1}^{N} v_m(\mathbf{x}_i, \omega) \sum_{k=1}^{N} \iint_{\Omega} \varphi_i(\mathbf{x})\varphi_k(\mathbf{x}) dxdy \\ &= \sum_{i=1}^{N} f_m(\mathbf{x}_i, \omega) \sum_{k=1}^{N} \iint_{\Omega} \varphi_i(\mathbf{x})\varphi_k(\mathbf{x}) dxdy, \end{aligned} \tag{17}$$

Consequentially, the matrix form of (17) is given by

$$(-\mathbf{Q} + k_m^2(\omega)\mathbf{P})\mathbf{v}_m(\omega) = \mathbf{P}\mathbf{f}_m(\omega), \tag{18}$$

where

$$[\mathbf{Q}]_{ik} = \iint_{\Omega} \nabla\varphi_i(\mathbf{x})\nabla\varphi_k(\mathbf{x})dxdy, \tag{19}$$

$$[\mathbf{P}]_{ik} = \iint_{\Omega} \varphi_i(\mathbf{x})\varphi_k(\mathbf{x})dxdy, \tag{20}$$

$$\mathbf{v}_m(\omega) = [v_m(\mathbf{x}_1,\omega), v_m(\mathbf{x}_2,\omega), ..., v_m(\mathbf{x}_N,\omega)]^T, \tag{21}$$

$$\mathbf{f}_m(\omega) = [f_m(\mathbf{x}_1,\omega), f_m(\mathbf{x}_2,\omega), ..., f_m(\mathbf{x}_N,\omega)]^T. \tag{22}$$

Each element of the system matrices $\mathbf{Q}$ and $\mathbf{P}$ is computed via the basis functions. The vector $\mathbf{v}_m(\omega)$ denotes the scattered field of the mth wave mode at the particular frequency ω over N mesh points. The vector $\mathbf{f}_m(\omega)$ denotes the approximated source of the mth mode due to the damage at frequency ω over N mesh points. Note that in the FEM approximation, the basis functions are piecewise functions that have limited local spatial support, and we only have to calculate the correlation result between basis functions that have close spatial support. Furthermore, the mesh points are assigned as the vertexes of local triangular elements, and only the correlation within the same local triangular are taken into account. Hence, the whole area is divided into small finite elements. We only need to calculate the parameters for each element and accumulate all local results to form the global matrices. This avoids to solve the PDE analytically, but still retains the accuracy of the solutions to some extent according to the density of mesh points. Via the FEM, the original PDE system model is transformed into a discrete linear model, which is ready for damage localization.

We remark that due to the choice of the basis functions, the matrices $\mathbf{Q}$ and $\mathbf{P}$ are symmetric, positive semi-definite, and block-diagonal sparse. Once the mesh points and the basis functions are determined, the matrices $\mathbf{Q}$ and $\mathbf{P}$ can be automatically obtained by (19) and (20). The matrices $\mathbf{Q}$ and $\mathbf{P}$ are different from the *stiffness* and *mass* matrices in the traditional system models based on the motion equations [8]. The *stiffness* and *mass* matrices correlate with the physical configuration of the structure, and an actual damage would locally change the elements of these matrices. Therefore, the system model has to be refined according to measurements. On the other hand, the proposed system model is based on the wave propagating equation, and the damage is modeled as an extended source from the damaged boundaries. Since the wave propagation in an isotropic solid media yields constant patterns, the matrices $\mathbf{Q}$ and $\mathbf{P}$ would not change despite the existence of the damages. It relieves the burden of updating these two matrices.

IV. The Sparse Damage Localization Algorithm

With the observation model (10) and the approximated system model (18), the damage localization can be achieved through estimating the nonzero values of the vector $\mathbf{f}_m(\omega)$. This kind of problem is called the inverse problem, as we try to infer unknown parameters of a system given the system response and system model.

To recover the field vector $\mathbf{v}_m(\omega)$ and the approximated damages vector $\mathbf{f}_m(\omega)$ with very few observations is difficult, since it is a highly underdetermined problem. In this paper, the damages are assumed to be small and spatially sparse. Therefore, the vector $\mathbf{f}_m(\omega)$ is sparse. The inverse problem is solved by taking the sparse feature of $\mathbf{f}_m(\omega)$ as a ℓ_1 regularization term into account. Thus, the nonzero elements of $\mathbf{f}_m(\omega)$ indicate the location and the scattering effects of the damages. Using the measurements from J sensors and the approximated system model (18), the damage localization is equivalent to solving the following optimization problem

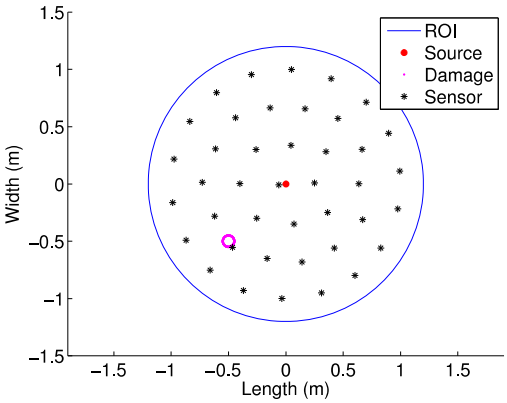

Fig. 1. The experimental setup

$$\min_{\mathbf{v}_m(\omega),\mathbf{f}_m(\omega)} \sum_{j=1}^{J} \left\|\bar{v}_m(\mathbf{x}_j,\omega) - v_m(\mathbf{x}_j,\omega)\right\|_2^2 + \lambda_1 \left\|\mathbf{f}_m(\omega)\right\|_1 + \lambda_2 \left\|(-\mathbf{Q} + k_m^2(\omega)\mathbf{P})\mathbf{v}_m(\omega) - \mathbf{P}\mathbf{f}_m(\omega)\right\|_2^2, \tag{23}$$

where λ_1 and λ_2 are the regularization parameters that balance the sparsity and the system fitting error. The first term of (23) minimizes the observation noise, the second term forces the sparsity of $\mathbf{f}_m(\omega)$, and the last term minimizes the system model fitting error. We solve this problem by employing convex optimization toolbox CVX [20] and perform cross validation.

Note that with the accurately estimated vector $\mathbf{v}_m(\omega)$, the damage region can be distinguished, as the damages would cause strong scattered filed response around it. We define a threshold γ, and pick up the elements in $\mathbf{v}_m(\omega)$ by comparing their values to the threshold

$$|\mathbf{v}_m(\omega)| > \gamma. \tag{24}$$

As a result, the mesh points with field value higher than the threshold are then bounded by a minimum circle. The circle indicates the region where the damages occur with a high probability.

We remark that the proposed method differs from the conventional damage identification based on the motion models [2, 8, 9] in two fold: i) the system matrices of the proposed method do not vary before and after damage occurs, thus we do not have to update them; ii) in the proposed method, the damage related parameters in the model are linearly related to

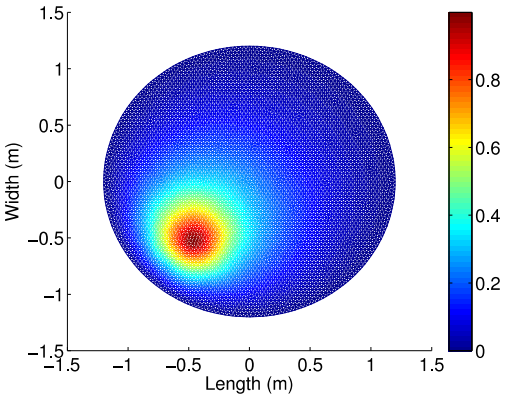

Fig. 2. Recovered field $\mathbf{v}_m(\omega)$ at SNR $= 20\,\mathrm{dB}$ (The color bar denotes the normalized frequency response)

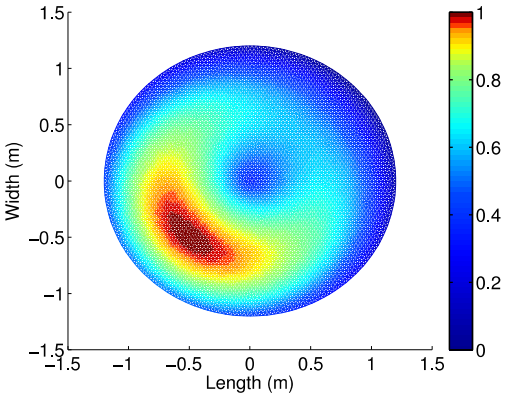

Fig. 3. The damage index of the DAS method at SNR $= 20\,\mathrm{dB}$ (The color bar denotes the normalized damage index)

the measurements. Consequentially, the spatial sparsity characteristics of the damages can be directly utilized and combined with the system model and measurements for solving the inverse problem.

V. Numerical Results

In this section, the performance of the proposed algorithm is evaluated by numerical experiments. The wave propagation in an aluminum plate is mimicked. The experimental setup is illustrated in Fig. 1. The region of interest (ROI) is a sphere with radius of $1.2\,\mathrm{m}$ and centered at the origin. The absorbing boundary condition is applied for the edge of the plate for the simulation. The thickness of the plate is $1\,\mathrm{mm}$, and the source excites at the origin. A through-thickness hole with radius of $0.05\,\mathrm{m}$ centered at $(-0.5\,\mathrm{m}, -0.5\,\mathrm{m})$ is employed as a damage. As shown in Fig. 1, several sensors ($J = 41$) are uniformly deployed in the ROI. The mesh of the FEM is composed of triangles with an average edge of $0.02\,\mathrm{m}$. Hence, the number of the mesh points is 5609 in total, and the length N of $\mathbf{v}_m(\omega)$ and $\mathbf{f}_m(\omega)$ is 5609. The damage hole scatters the incident waves, and the responses are captured by all the sensors. The measurements are corrupted by AWGN, and used as inputs for the proposed method. The measurements from the intact aluminum plate are employed by the proposed methods as well.

Fig. 2 shows the recovered field $\mathbf{v}_m(\omega)$ generated by the proposed method in the ROI. The damage region around $(-0.5\,\mathrm{m}, -0.5\,\mathrm{m})$ can be distinguished from other regions by the amplitude of the recovered field $\mathbf{v}_m(\omega)$. The proposed method is compared with a widely used delay-and-sum (DAS) method [21]. The DAS method is a response-based method that only depends on the measurements. In the DAS, the ROI is separated into small pixels centering at the mesh points, and a correlation-based damage index is calculated for each pixel. We test the DAS method with the same data, and the number of the pixels is the same as the mesh points used in the proposed method. The result is plotted in Fig. 3, where the damage index can be viewed as the probability of damage occurrence. Comparing Fig. 2 with Fig. 3, we can find that the region with high suspect probability of damage in the DAS method spreads out, while the results of the proposed method more closely locate around the damage.

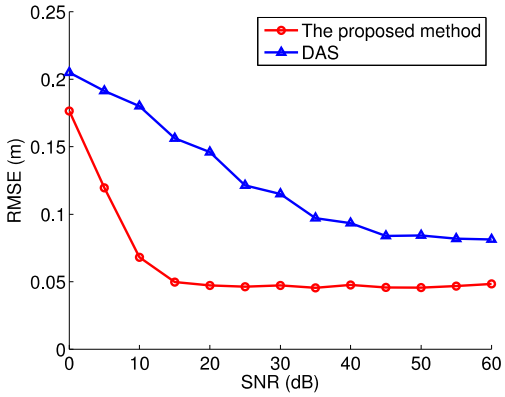

Fig. 4. Comparison of RMSE with the center of damage between the proposed method and the DAS method

Further, we compare the localizing performance between the two methods at different signal-to-noise ratios (SNR). SNR is defined as

$$\mathrm{SNR} = 10 \log \frac{v_m(\mathbf{x}_j, \omega)}{n(\mathbf{x}_j, \omega)} \tag{25}$$

For the proposed method, nodes with high amplitude values are picked up from the recovered field, threshold is employed as 95% of the maximum value. For the DAS method, we extract the nodes with damage probability higher than 95%. All nodes extracted from the two methods are bounded by a minimum covering circle, respectively. Centers of the two circles are compared with the center of the damage region and calculate the root-mean-square-error (RMSE), respectively. For each SNR, we perform 1000 Monte Carlo trial for both algorithms. Mark the center of the damage as (x_r, y_r), mark the center of region estimated with the ith Monte Carlo trial as (x_i, y_i), denote n_{mont} as the total number of Monte Carlo

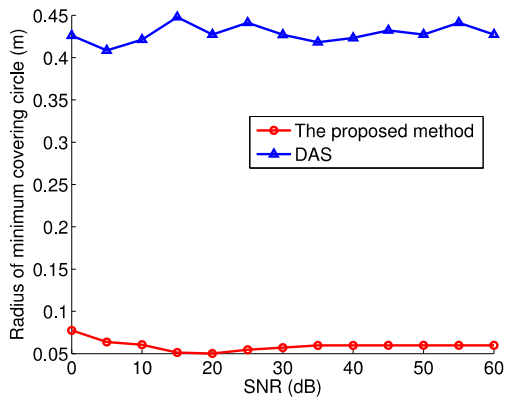

Fig. 5. Comparison of radius of minimum covering circle between the proposed method and the DAS method

trials. RMSE is defined as the

$$\mathrm{RMSE} = \sqrt{\frac{\sum_{i=1}^{n_{mont}} (x_i - x_r)^2 + (y_i - y_r)^2}{n_{mont}}} \tag{26}$$

The comparison of RMSE of the proposed method and the DAS method is plotted in Fig. 4. The proposed method maintains much less RMSE compared to the DAS method. Note that the result of the proposed method converge to around $0.05\,\mathrm{m}$ but not $0\,\mathrm{m}$. This is due to the fact that damage boundary closer to the source cause stronger scattered field, and the extracted nodes might not spread evenly around the center of the damage. By employing a larger threshold the RMSE of the proposed method can be reduced. Moreover, Fig. 5 shows the radius of the circles for covering the nodes of the two methods, respectively. The radius of the proposed method is smaller than the one of the DAS method in Fig. 5.

VI. Conclusions

In this paper, we proposed a model-based sparse damage localization algorithm. We construct a system model based on the wave propagation characteristics. The FEM approximates the model to relax the complexity. By introducing a WSN in our work, we achieve the observations with distributed sensors. Spatially sparse damages are related to the unknown sparse parameters in our model and we force ℓ_1 norm regularization to solve the optimization problem for localizing. Numerical results show that our method is superior to a commonly used response-based method (e.g. the DAS method).

Acknowledgement

Part of the work was supported by the National Nature Science Foundation of China (No. 61301223), the Nature Science Foundation of Shanghai (No. 13ZR1421800).

References

[1] S. W. Doebling, C. R. Farrar, M. B. Prime *et al.*, "A summary review of vibration-based damage identification methods," *Shock and vibration digest*, vol. 30, no. 2, pp. 91–105, 1998.

[2] W. Fan and P. Qiao, "Vibration-based damage identification methods: a review and comparative study," *Structural Health Monitoring*, vol. 10, no. 1, pp. 83–111, 2011.

[3] J. P. Lynch and K. J. Loh, "A summary review of wireless sensors and sensor networks for structural health monitoring," *Shock and Vibration Digest*, vol. 38, no. 2, pp. 91–130, 2006.

[4] Z. Su and L. Ye, *Identification of damage using Lamb waves: from fundamentals to applications*. Springer, 2009, vol. 48.

[5] Z. Su, L. Ye, and Y. Lu, "Guided Lamb waves for identification of damage in composite structures: A review," *Journal of sound and vibration*, vol. 295, no. 3, pp. 753–780, 2006.

[6] A. Raghavan and C. E. Cesnik, "Review of guided-wave structural health monitoring," *Shock and Vibration Digest*, vol. 39, no. 2, pp. 91–116, 2007.

[7] M. Ghasemi and M. Ghafory-Ashtiany, "Damage detection method by using inverse solution of equations of motion in frequency domain," in *Proc. 15th WCEE*, Lisbon, Portugal, September 2012.

[8] M. I. Friswell, "Damage identification using inverse methods," *Philosophical Transactions of the Royal Society A: Mathematical, Physical and Engineering Sciences*, vol. 365, no. 1851, pp. 393–410, 2007.

[9] C. C. Ciang, J. R. Lee, and H. J. Bang, "Structural health monitoring for a wind turbine system: a review of damage detection methods," *Measurement Science and Technology*, vol. 19, no. 12, pp. 1–20, 2008.

[10] J. L. Rose, *Ultrasonic waves in solid media*. Cambridge university press, 2004.

[11] S. C. Brenner and R. Scott, *The mathematical theory of finite element methods*. Springer, 2008, vol. 15.

[12] J. E. Michaels, S. J. Lee, A. J. Croxford, and P. D. Wilcox, "Chirp excitation of ultrasonic guided waves," *Ultrasonics*, vol. 53, no. 1, pp. 265–270, 2013.

[13] J. B. Harley and J. M. Moura, "Sparse recovery of the multimodal and dispersive characteristics of Lamb waves," *The Journal of the Acoustical Society of America*, vol. 133, no. 5, pp. 2732–2745, 2013.

[14] L. De Marchi, M. Ruzzene, B. Xu, E. Baravelli, and N. Speciale, "Warped basis pursuit for damage detection using Lamb waves," *IEEE Transactions on Ultrasonics, Ferroelectrics and Frequency Control*, vol. 57, no. 12, pp. 2734–2741, 2010.

[15] D. Colton and R. Kress, *Inverse acoustic and electromagnetic scattering theory*. Springer, 2012, vol. 93.

[16] T. Grahn, "Lamb wave scattering from a circular partly through-thickness hole in a plate," *Wave Motion*, vol. 37, no. 1, pp. 63–80, 2003.

[17] Q. Deng and Z. Yang, "Scattering of s0 Lamb mode in plate with multiple damage," *Applied Mathematical Modelling*, vol. 35, no. 1, pp. 550–562, 2011.

[18] S. Chaillat and G. Biros, "FaIMS: A fast algorithm for the inverse medium problem with multiple frequencies and multiple sources for the scalar Helmholtz equation," *Journal of Computational Physics*, vol. 231, no. 12, pp. 4403–4421, 2012.

[19] J. Gubernatis, E. Domany, J. Krumhansl, and M. Huberman, "The Born approximation in the theory of the scattering of elastic waves by flaws," *Journal of Applied Physics*, vol. 48, no. 7, pp. 2812–2819, 1977.

[20] M. Grant and S. Boyd, "CVX: Matlab software for disciplined convex programming, version 2.1," http://cvxr.com/cvx, Mar. 2014.

[21] J. E. Michaels, A. J. Croxford, and P. D. Wilcox, "Imaging algorithms for locating damage via in situ ultrasonic sensors," in *Proc. IEEE SAS*, Atlanta, GA, USA, February 2008, pp. 63–67.